

## Study on Vibration Characteristics and Measuring Method for Farm Machinery

Eiji INOUE\*<sup>1</sup>, Ryozi NOGUCHI\*<sup>2</sup> and Young Keun KIM\*<sup>1</sup>

\*<sup>1</sup> Faculty of Agriculture, Kyushu University (Fukuoka, Fukuoka, 812-81 Japan)

\*<sup>2</sup> Institute of Agricultural and Forest Engineering, University of Tsukuba  
(Tsukuba, Ibaraki, 305 Japan)

### Abstract

Driving simulation using the motion equations based on the 3-dimensional dynamic model of the rubber crawler traction system was performed under various conditions. The location arrangement of track rollers was estimated through the experimental results and driving simulation. Components of vibrational acceleration of the rubber crawler traction system with 6 degrees of freedom could be measured individually and accurately using the new measuring method proposed by the authors. Accuracy of translational components of vibrational acceleration improved remarkably compared with the conventional measuring method. Motion equations and frequency transfer function of a riding tractor with rotary tillage equipment were proposed. Simulated data of frequency response were compared with measured data of forced vibration experiment to determine the validity for tractor's dynamic model.

**Discipline:** Agricultural machinery

**Additional key words:** dynamic model, rubber crawler, simulation, components with 6 degrees of freedom, riding tractor

### Introduction

Analysis of vibrations of farm machinery is very important for optimum design from the viewpoint of human engineering. In particular, analysis of vibrations of combine harvester and riding tractor among farm machines contributes to the improvement of farm operation efficiency. Furthermore, it is necessary to define the components of vibrational acceleration with 6 degrees of freedom in order to investigate the vibration characteristics of farm machinery. Formerly, a measuring method using 9 units of accelerometers was proposed by Ono et al.<sup>(8)</sup>. However, this method was found to hamper the calculation of translational components. Therefore, a new measuring method was required for improving the accuracy of the translational components.

In this paper, the vibration characteristics of a rubber crawler system for a combine harvester were analyzed in order to devise a design concept for the optimum location arrangement of track rollers by minimizing machine vibrations<sup>(1-4)</sup>. Furthermore, a new measuring method of components of vibrational acceleration with 6 degrees of freedom was

proposed by the authors<sup>(5)</sup>. Finally, the riding tractor's vibration characteristics associated with the rotary tillage resistance were analyzed<sup>(6,7)</sup>.

### Analysis of vibration characteristics of agricultural rubber crawler system

The Voigt model composed of the dynamic spring constant,  $k$ , and viscous damping coefficient,  $C$ , was applied to construct a 3-dimensional dynamic model of a rubber crawler traction system for a combine harvester driving on a solid horizontal surface (Fig. 1).

The dynamic spring constant and viscous damping coefficient of the rubber crawler beneath the track rollers in actual driving can be expressed as periodical functions of time  $t$ <sup>(3)</sup>, where,

$k_{Li}(t)$ ,  $k_{Ri}(t)$ : dynamic spring constant (kN/m),  
 $C_{Li}(t)$ ,  $C_{Ri}(t)$ : viscous damping coefficient (kN·s/m),  
 $\phi$ : pitch angle (rad),  $\psi$ : roll angle (rad),  
 $I_y$ : pitch moment of inertia (kgm<sup>2</sup>),  
 $I_x$ : roll moment of inertia (kgm<sup>2</sup>).

As a result of the measurement performed when the system is placed on a shaker within a certain range of frequency,  $C_n(t)$  and  $k_n(t)$  of the rubber

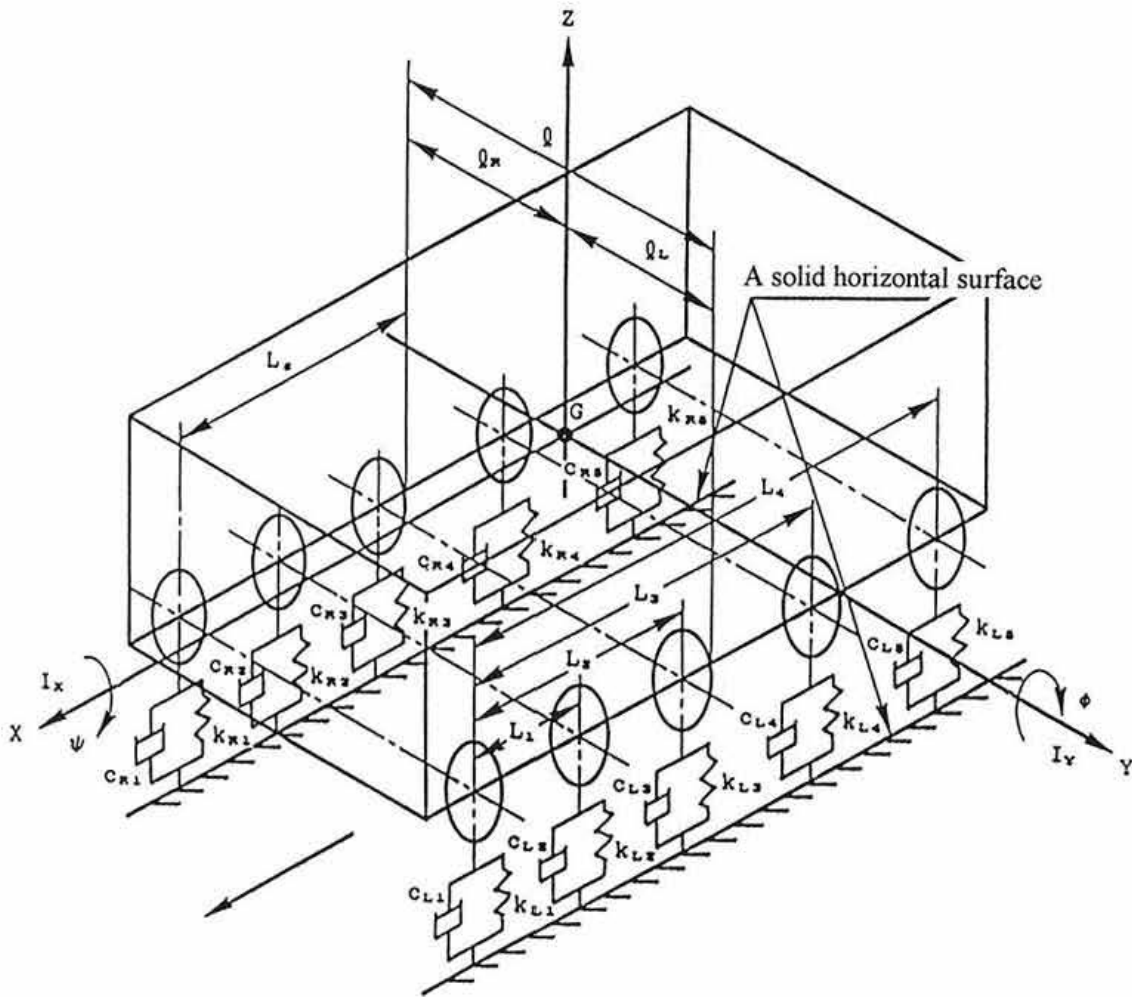


Fig. 1. Dynamic 3-dimensional model

crawler can be expressed in the form of Fourier series as follows:

$$k_n(t) = \frac{a_0}{2} + \sum_{j=1}^{N/2-1} (a_j \cos j(2\pi ft + \alpha) + b_j \sin j(2\pi ft + \alpha)) + \frac{a_{N/2}}{2} \cos \frac{N}{2} (2\pi ft + \alpha) \dots (1)$$

$$c_n(t) = \frac{c_0}{2} + \sum_{j=1}^{N/2-1} (c_j \cos j(2\pi ft + \alpha) + d_j \sin j(2\pi ft + \alpha)) + \frac{c_{N/2}}{2} \cos \frac{N}{2} (2\pi ft + \alpha) \dots (2)$$

Motion equations are obtained based on the model shown in Fig. 1, where,

$$L_g = l_1, L_g - L_1 = l_2, L_g - L_2 = l_3 \dots, L_g - L_{i-1} = l_i \dots (3)$$

In the case of bouncing:

$$M\ddot{z} + z \sum_{i=1}^n (k_{Li}(t) + k_{Ri}(t)) + \phi \sum_{i=1}^n (k_{Li}(t)l_i + k_{Ri}(t)l_i) + \psi \sum_{i=1}^n (k_{Li}(t)lL - k_{Ri}(t)lR) + \dot{z} \sum_{i=1}^n (C_{Li}(t) + C_{Ri}(t)) + \dot{\phi} \sum_{i=1}^n (C_{Li}(t)l_i + C_{Ri}(t)l_i) + \dot{\psi} \sum_{i=1}^n (C_{Li}(t)lL - C_{Ri}(t)lR) = Mg \dots (4)$$

In the case of pitching:

$$\begin{aligned}
 I_y \ddot{\phi} + \phi \sum_{i=1}^n (kLi(t)li^2 + kRi(t)li^2) + z \sum_{i=1}^n (kLi(t)li \\
 + kRi(t)li) + \psi \sum_{i=1}^n (kLi(t)lilL - kRi(t)lilR) \\
 + \dot{\phi} \sum_{i=1}^n (CLi(t)li^2 + CRi(t)li^2) + \dot{z} \sum_{i=1}^n (CLi(t)li \\
 + CRi(t)li) + \dot{\psi} \sum_{i=1}^n (CLi(t)lilL - CRi(t)lilR) = 0
 \end{aligned}
 \tag{5}$$

In the case of rolling:

$$\begin{aligned}
 I_x \ddot{\psi} + \psi \sum_{i=1}^n (kLi(t)lL^2 + kRi(t)lR^2) + z \sum_{i=1}^n (kLi(t)lL \\
 + kRi(t)lR) + \phi \sum_{i=1}^n (kLi(t)lilL - kRi(t)lilR) \\
 + \dot{\psi} \sum_{i=1}^n (CLi(t)lL^2 + CRi(t)lR^2) + \dot{z} \sum_{i=1}^n (CLi(t)lL \\
 + CRi(t)lR) + \dot{\phi} \sum_{i=1}^n (CLi(t)lilL - CRi(t)lilR) = 0
 \end{aligned}
 \tag{6}$$

These equations are obtained by the determination of spring constants and viscous damping coefficients in only the vertical direction<sup>3)</sup>. However, estimation of the machine vibration associated with pitching and bouncing can be adequately represented as shown in Fig. 2.

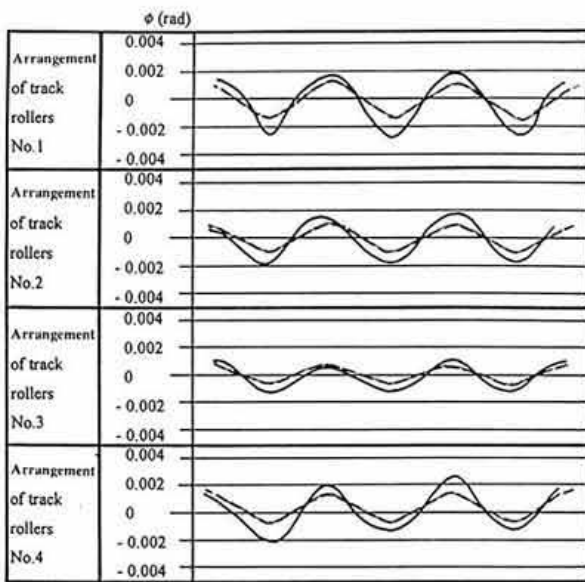
**Measuring method of components of vibrational acceleration with 6 degrees of freedom**

1) *Measuring theory*

Accelerometers which are fixed to a rigid body and not located in the center of gravity of the rigid body sense both translational and rotational components when the rigid body is moving. Therefore, an expanded new measuring theory using 12 units of accelerometers by the addition of further 3 units of accelerometers was proposed by the authors<sup>5)</sup>. By this new measuring theory, components of acceleration with 6 degrees of freedom can be measured individually and accurately. The arrangement of the accelerometers is shown in Fig. 3.

Coordinates of the accelerometers (X<sub>1</sub> ~ Z<sub>4</sub>) are as follows:

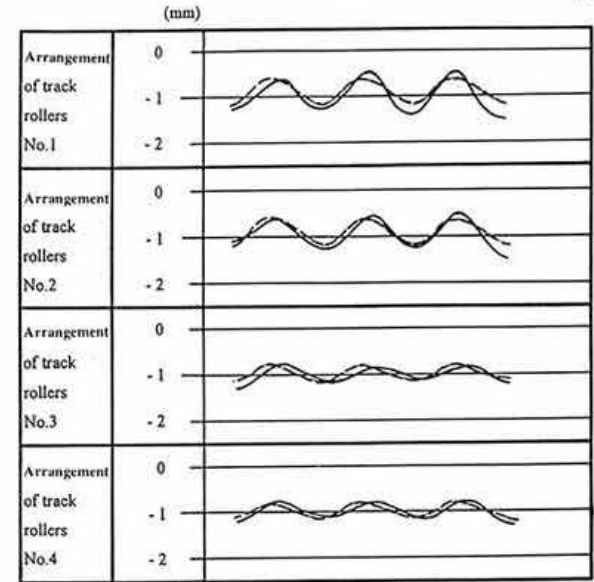
- X1: (h<sub>1x</sub>, h<sub>1y</sub>, h<sub>1z</sub>)    Y1: (m<sub>1x</sub>, m<sub>1y</sub>, m<sub>1z</sub>)    Z1: (n<sub>1x</sub>, n<sub>1y</sub>, n<sub>1z</sub>)
- X2: (h<sub>2x</sub>, h<sub>2y</sub>, h<sub>2z</sub>)    Y2: (m<sub>2x</sub>, m<sub>2y</sub>, m<sub>2z</sub>)    Z2: (n<sub>2x</sub>, n<sub>2y</sub>, n<sub>2z</sub>)
- X3: (h<sub>3x</sub>, h<sub>3y</sub>, h<sub>3z</sub>)    Y3: (m<sub>3x</sub>, m<sub>3y</sub>, m<sub>3z</sub>)    Z3: (n<sub>3x</sub>, n<sub>3y</sub>, n<sub>3z</sub>)
- X4: (h<sub>4x</sub>, h<sub>4y</sub>, h<sub>4z</sub>)    Y4: (m<sub>4x</sub>, m<sub>4y</sub>, m<sub>4z</sub>)    Z4: (n<sub>4x</sub>, n<sub>4y</sub>, n<sub>4z</sub>)



Driving speed : 0.672 m/s

———— : Experimental results  
 - - - - - : Simulated results

Pitching



Driving speed : 0.672 m/s

———— : Experimental results  
 - - - - - : Simulated results

Bouncing

Fig. 2. Experimental and simulated results of pitch angle and bouncing

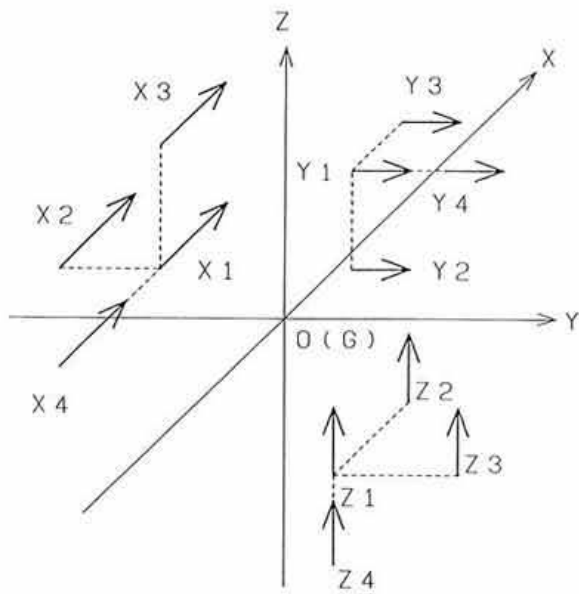


Fig. 3. Arrangement of accelerometers

where,

$$\begin{aligned} h_{1x} = h_{2x} = h_{3x} & \quad m_{1x} = m_{2x} = m_{4x} & \quad n_{1x} = n_{3x} = n_{4x} \\ h_{1y} = h_{3y} = h_{4y} & \quad m_{1y} = m_{2y} = m_{3y} & \quad n_{1y} = n_{2y} = n_{4y} \\ h_{1z} = h_{2z} = h_{4z} & \quad m_{1z} = m_{3z} = m_{4z} & \quad n_{1z} = n_{2z} = n_{3z} \end{aligned} \quad \dots \dots \dots (8)$$

The translational accelerations (X direction ( $\alpha_{gx}$ ), Y direction ( $\alpha_{gy}$ ), Z direction ( $\alpha_{gz}$ )) and rotation accelerations (roll ( $\theta_x$ ), pitch ( $\theta_y$ ), yaw ( $\theta_z$ )) are obtained by the equations (9) and (10):

$$\begin{bmatrix} \alpha_{gx} \\ \alpha_{gy} \\ \alpha_{gz} \end{bmatrix} = \begin{bmatrix} 1 + \frac{h_{1z}}{h_2} + \frac{h_{1y}}{h_1} + \frac{h_{1x}}{h_7} & & 0 \\ 0 & 1 + \frac{m_{1x}}{h_4} + \frac{m_{1z}}{h_3} + \frac{m_{1y}}{h_8} & \\ 0 & & 0 \end{bmatrix} \begin{bmatrix} \alpha_{1x} \\ \alpha_{1y} \\ \alpha_{1z} \end{bmatrix} + \begin{bmatrix} 0 \\ 0 \\ 1 + \frac{n_{1y}}{h_6} + \frac{n_{1x}}{h_5} + \frac{n_{1z}}{h_9} \end{bmatrix} \begin{bmatrix} \alpha_{2x} \\ \alpha_{2y} \\ \alpha_{2z} \end{bmatrix} \quad \dots \dots \dots (9)$$

$$\begin{aligned} & - \begin{bmatrix} -\frac{h_{1z}}{h_2} & 0 & 0 \\ 0 & -\frac{m_{1x}}{h_4} & 0 \\ 0 & 0 & -\frac{n_{1y}}{h_6} \end{bmatrix} \begin{bmatrix} \alpha_{2x} \\ \alpha_{2y} \\ \alpha_{2z} \end{bmatrix} \\ & + \begin{bmatrix} -\frac{h_{1y}}{h_1} & 0 & 0 \\ 0 & -\frac{m_{1z}}{h_3} & 0 \\ 0 & 0 & -\frac{n_{1x}}{h_5} \end{bmatrix} \begin{bmatrix} \alpha_{3x} \\ \alpha_{3y} \\ \alpha_{3z} \end{bmatrix} \\ & + \begin{bmatrix} -\frac{h_{1x}}{h_7} & 0 & 0 \\ 0 & -\frac{m_{1y}}{h_8} & 0 \\ 0 & 0 & -\frac{n_{1z}}{h_9} \end{bmatrix} \begin{bmatrix} \alpha_{4x} \\ \alpha_{4z} \\ \alpha_{4z} \end{bmatrix} \dots \dots \dots (9) \end{aligned}$$

where,

$$h_7 = h_{4x} - h_{1x}, h_8 = m_{4y} - m_{1y}, h_9 = n_{4z} - n_{1z}$$

$$\begin{bmatrix} \theta_x \\ \theta_y \\ \theta_z \end{bmatrix} = \frac{1}{2} \begin{bmatrix} 0 & -1/h_3 & -1/h_6 \\ -1/h_2 & 0 & -1/h_5 \\ -1/h_1 & -1/h_4 & 0 \end{bmatrix} \begin{bmatrix} \alpha_{1x} \\ \alpha_{1y} \\ \alpha_{1z} \end{bmatrix} + \begin{bmatrix} 0 & 0 & 1/h_6 \\ 1/h_2 & 0 & 0 \\ 0 & 1/h_4 & 0 \end{bmatrix} \begin{bmatrix} \alpha_{2x} \\ \alpha_{2y} \\ \alpha_{2z} \end{bmatrix} + \begin{bmatrix} 0 & 1/h_3 & 0 \\ 0 & 0 & 1/h_5 \\ 1/h_1 & 0 & 0 \end{bmatrix} \begin{bmatrix} \alpha_{3x} \\ \alpha_{3y} \\ \alpha_{3z} \end{bmatrix} \dots \dots \dots (10)$$

Accelerometers required to calculate the acceleration components are shown in Table 1.

2) Experiment and results

The rubber crawler system of a Japanese type combine harvester was reconstructed and used for the experiment. The instrument unit equipped with

Table 1. Accelerometers for measurement of 6 degrees of freedom

	X1	X2	X3	X4	Y1	Y2	Y3	Y4	Z1	Z2	Z3	Z4
$\theta_X$					○		○		○	○		
$\theta_Y$	○	○							○		○	
$\theta_Z$	○		○		○	○						
$\omega_X^2$	○			○	○			○	○			○
$\omega_Y^2$	○			○	○			○	○			○
$\omega_Z^2$	○			○	○			○	○			○
$\alpha_{gx}$	○	○	○	○								
$\alpha_{gy}$					○	○	○	○				
$\alpha_{gz}$									○	○	○	○

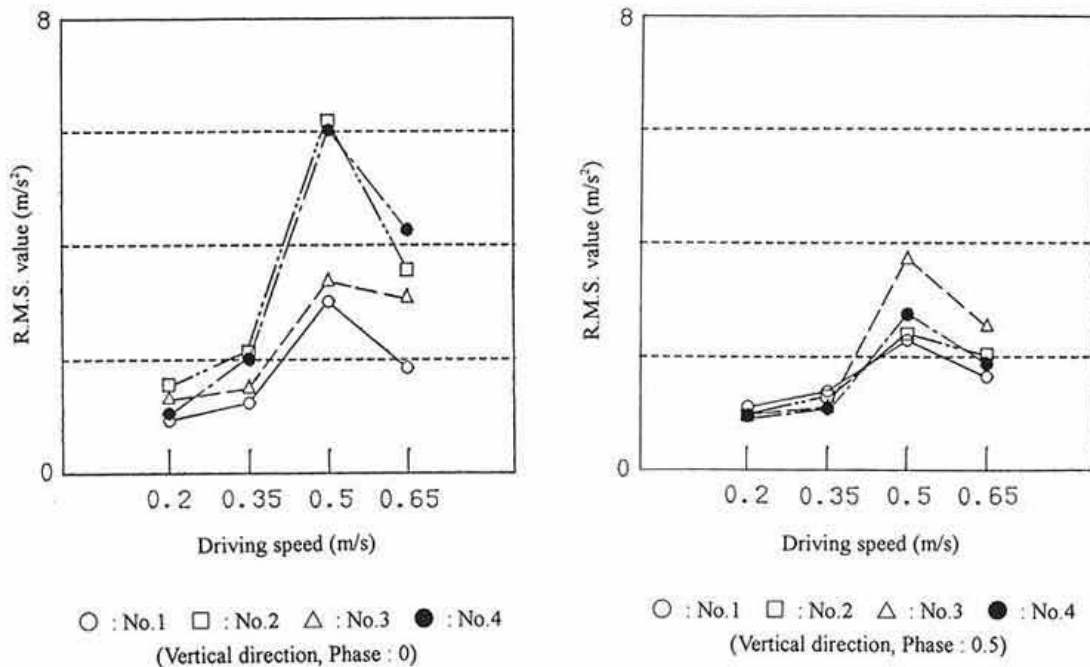


Fig. 4. R.M.S. values of acceleration

12 units of accelerometers was mounted on the rear section of the tested rubber crawler system. Fig. 4 shows an example of the R.M.S. values of acceleration in the vertical direction. In the vertical direction, the higher the driving speed, the larger the R.M.S. values, while the larger the lug phase, the smaller the R.M.S. values. A peak of R.M.S. values appears near the 0.5 m/s because the natural frequency of the rubber crawler system approximately corresponds to a frequency of vibration caused by track rollers passing through the lugs or metal core<sup>4)</sup>.

**Analysis of vibration characteristics of a riding tractor with rotary tillage equipment**

1) *Tractor dynamic model*

Tractor dynamic model<sup>7)</sup> has 3 degrees of freedom in the horizontal direction (x-axis direction), vertical direction (y-axis direction), and pitching direction ( $\phi$  direction) on the 2-dimension plane model shown in Fig. 5.

Condition without the deviation of rotary tillage resistance is considered to be balanced from the dynamic aspect. The equation of motion was controlled

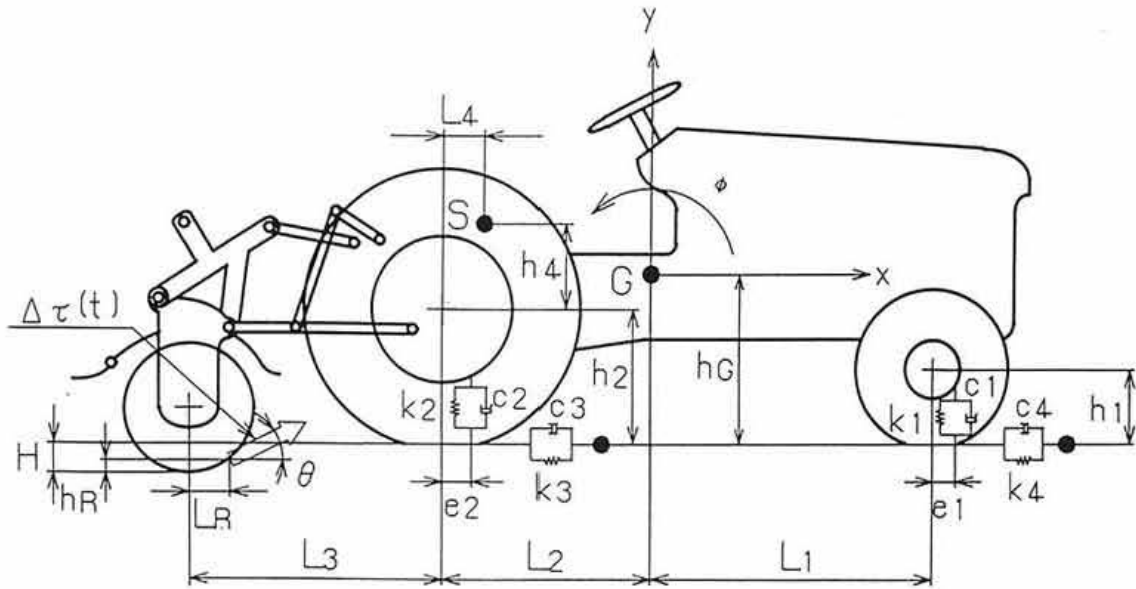


Fig. 5. Dynamic model of riding tractor with rotary tillage equipment

by Lagrange's equation. Small displacement deviation in the rotation around the center of gravity of the tractor dynamic model is defined by the following equation:

$$\begin{aligned} X_F &= X_G + h_G \phi & Y_F &= Y_G + (L_1 + e_1) \phi \\ X_R &= X_G + h_G \phi & Y_R &= Y_G - (L_2 - e_2) \phi \\ \dot{X}_F &= \dot{X}_G + h_G \dot{\phi} & \dot{Y}_F &= \dot{Y}_G + (L_1 + e_1) \dot{\phi} \\ \dot{X}_R &= \dot{X}_G + h_G \dot{\phi} & \dot{Y}_R &= \dot{Y}_G - (L_2 - e_2) \dot{\phi} \end{aligned} \quad \dots\dots\dots (11)$$

On the other hand, the relation between the center of gravity and the seat position of the tractor is defined as follows:

$$\begin{aligned} X_S &= X_G - (h_2 + h_3 - h_g) \phi \\ \dot{X}_S &= \dot{X}_G - (h_2 + h_3 - h_g) \dot{\phi} \\ Y_S &= Y_G - (L_2 + L_4 - h_g) \phi \\ \dot{Y}_S &= \dot{Y}_G - (L_2 + L_4 - h_g) \dot{\phi} \end{aligned} \quad \dots\dots\dots (12)$$

By using  $q_1 = X_G$ ,  $q_2 = Y_G$ ,  $q_3 = \phi$  and Lagrange's equation (13) ( $i = 1, 2, 3$ ), the dynamic model is defined by Eq. (14).

$$\frac{d}{dt} \left( \frac{\partial T}{\partial \dot{q}_i} \right) - \frac{\partial T}{\partial q_i} + \frac{\partial F}{\partial \dot{q}_i} + \frac{\partial U}{\partial q_i} = Q_i \quad \dots\dots\dots (13)$$

$$\begin{aligned} x_1 &= \dot{X}_G, & x_2 &= X_G, & x_3 &= \dot{Y}_G, & x_4 &= Y_G, \\ x_5 &= \dot{\phi}, & x_6 &= \phi, & y_1 &= \dot{X}_S, & y_2 &= X_G \end{aligned}$$

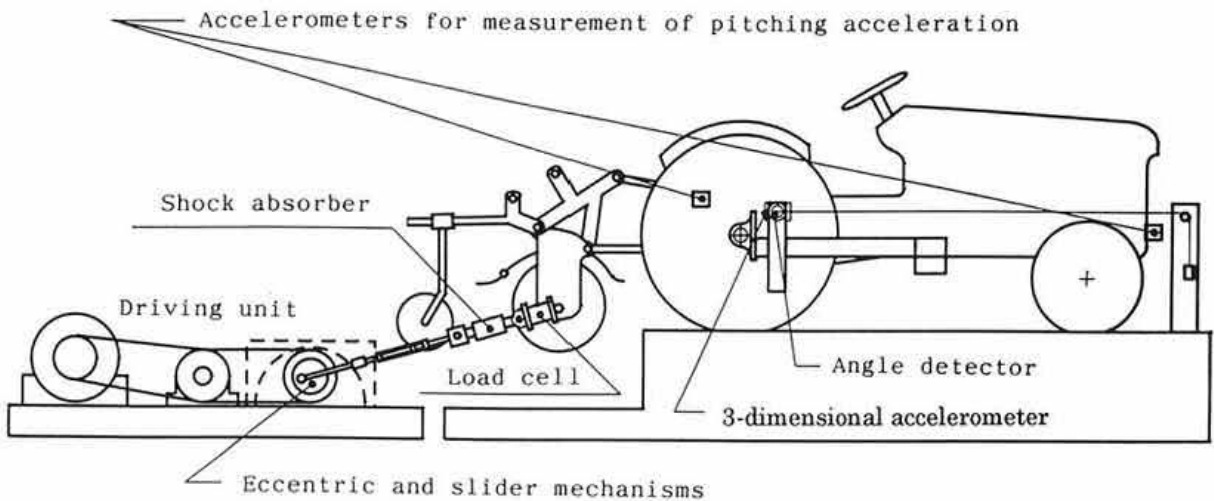


Fig. 6. Force shaker and forcing experiment of riding tractor

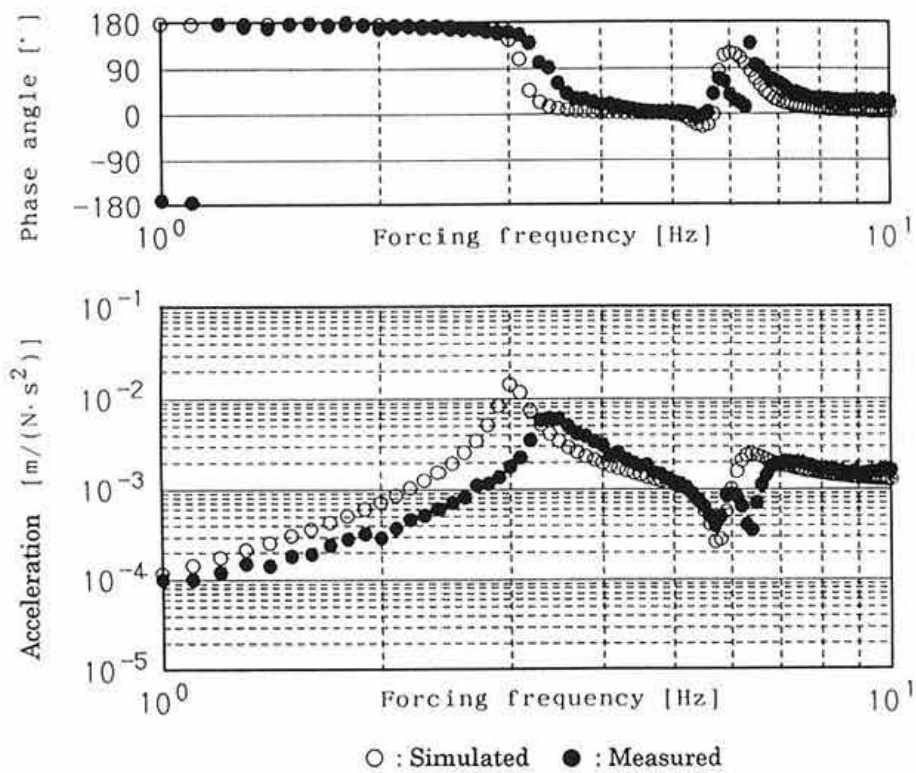


Fig. 7. Comparison between simulated and measured amplitude ratio and phase angle of acceleration in forward direction to the vibration force

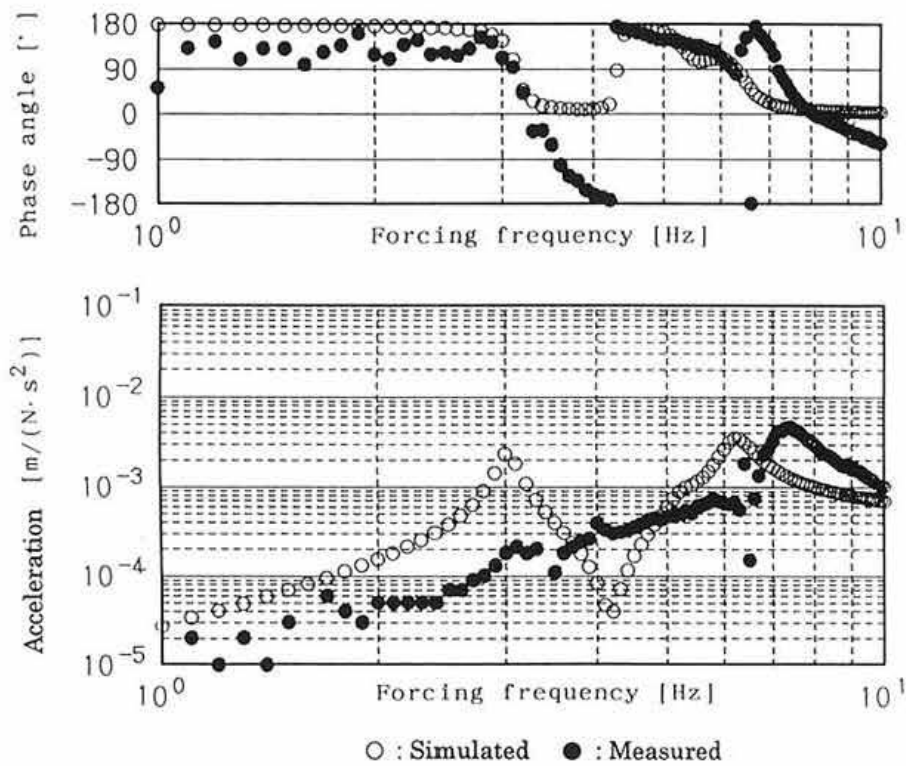


Fig. 8. Comparison between simulated and measured amplitude ratio and phase angle of acceleration in vertical direction to the vibration force

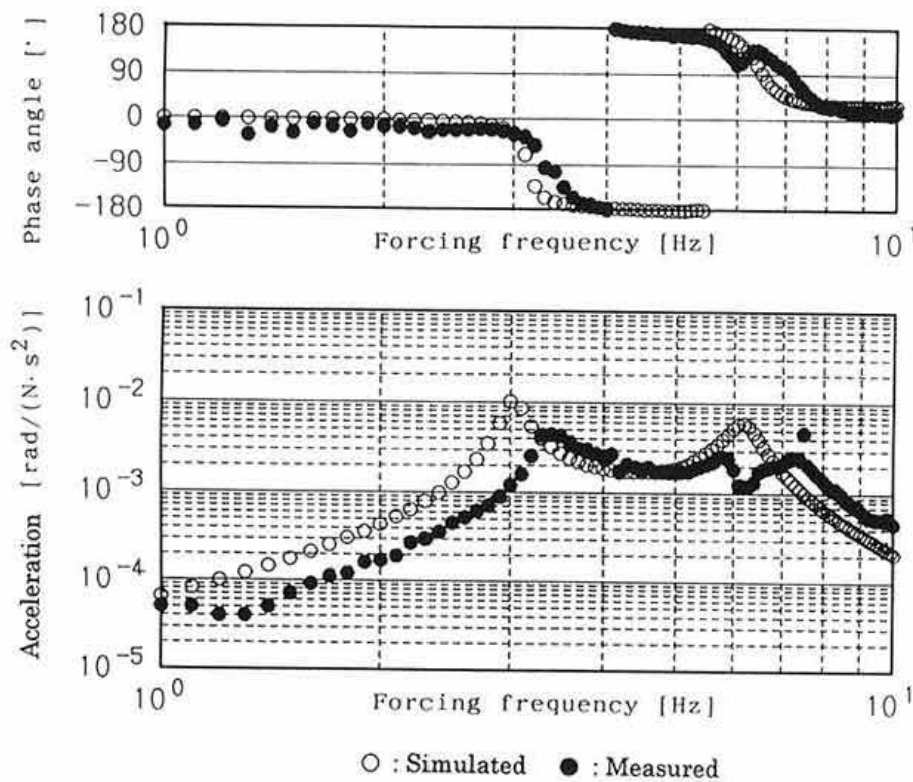


Fig. 9. Comparison between simulated and measured amplitude ratio and phase angle of acceleration in pitching direction to the vibration force

$$\begin{aligned}
 y_3 &= \dot{Y}s, \quad y_4 = Ys, \quad y_5 = \dot{\phi}, \quad y_6 = \phi, \\
 \mathbf{x} &= [x_1, x_2, x_3, x_4, x_5, x_6]^T \quad \mathbf{y} = [y_1, y_2, y_3, y_4, y_5, y_6]^T
 \end{aligned}
 \tag{14}$$

State equation and output equation for the tractor dynamic model are defined as linear differential equations by using a matrix and  $\tau(t)$  which is expressed as the reaction force of rotary tillage resistance.

$$\dot{\mathbf{x}} = \mathbf{A}\mathbf{x} + \mathbf{B}\tau(t) \quad \mathbf{y} = \mathbf{C}\mathbf{x} \tag{15}$$

Eq. (16) obtained by Laplace conversion from Eq. (15) is expressed as follows:

$$s\mathbf{X}(s) = \mathbf{A}\mathbf{X}(s) + \mathbf{B}\tau(s) \quad \mathbf{Y}(s) = \mathbf{C}\mathbf{X}(s) \tag{16}$$

As a result, the frequency transfer function of the tractor dynamics  $\mathbf{Gfr}(s)(6 \times 1)$  with  $\tau(t)$  as input and  $\mathbf{Y}(s)$  as output is expressed as follows:

$$\mathbf{Gfr}(s) = \mathbf{Y}(s)/\tau(s) = \mathbf{C}(s\mathbf{E} - \mathbf{A})^{-1}\mathbf{B} \tag{17}$$

Then the frequency transfer function after the change of the angle velocity  $\omega$  is determined by Eq. (17).

### 2) Vibration experiment and discussion

Forced vibration experiment of a tractor with rotary tillage equipment was conducted as shown in Fig. 6. The force shaker can impart an artificial vibration force to the tractor as the periodical forced vibration occurring from the rotary tillage equipment. Then forced vibration experiment by using sine curve based on the sweep vibration method was carried out in the frequency range between 1.0 Hz and 10.0 Hz by 1 Hz.

In the experiment, especially the peak of acceleration curve in the forward direction and pitching direction were observed at the same frequency in both simulation and experiment, as shown in Figs. 7, 8, 9 and it was demonstrated that a resonance frequency of the tractor could be obtained by using the dynamic model. However, a difference between simulation and experiment in the vertical direction along with the increase of forcing frequency can occur by the nonlinear phenomenon whereby some peaks not related to the forcing vibration frequency may be formed. Therefore, it was estimated that the nonlinear phenomenon affected in the same way the forward direction and pitching direction beyond

6.0 Hz in the forcing vibration frequency.

## Conclusion

A theoretical and experimental investigation was carried out in order to analyze the vibration characteristics, and develop a measuring method of vibrations for farm machinery. Based on this study, prediction of machine vibrations caused by the mechanical interaction between the rubber crawler and track rollers, and by the resistance of rotary tillage became possible. Furthermore, the measuring accuracy of components of vibrational acceleration with 6 degrees of freedom proposed by the authors improved for both translational and rotational components compared with the conventional measuring method.

## References

- 1) Inoue, E., Sakai, J. & Inaba, S. (1990): Basic studies on vibration characteristics of the rubber crawler system for farm machinery (Part 1). *J. JSAM*, **52**(2), 27–34.
- 2) Inoue, E., Sakai, J. & Inaba, S. (1990): Basic studies on vibration characteristics of the rubber crawler system for farm machinery (Part 2). *J. JSAM*, **52**(4), 29–36.
- 3) Inoue, E., Sakai, J. & Inaba, S. (1990): Basic studies on vibration characteristics of the rubber crawler system for farm machinery (Part 3). *J. JSAM*, **52**(5), 11–18.
- 4) Inoue, E., Sakai, J. & Inaba, S. (1990): Basic studies on vibration characteristics of the rubber crawler system for farm machinery (Part 4). *J. JSAM*, **52**(6), 19–26.
- 5) Inoue, E. et al. (1993): Measurement of 6 degrees of freedom components of acceleration in rubber crawler system. *J. JSAM*, **55**(5), 3–10.
- 6) Noguchi, R. et al. (1994): Basic studies on the dynamic characteristics of a riding tractor with rotary tiller (Part 1). *J. JSAM*, **56**(2), 11–22.
- 7) Noguchi, R. et al. (1994): Basic studies on the dynamic characteristics of a riding tractor with rotary tiller (Part 2). *J. JSAM*, **56**(3), 17–26.
- 8) Ono, K. et al. (1978): Total motion measurement and analysis on dummy head-neck system. *J. JSAE*, **14**, 26–32.

(Received for publication, March 31, 1997)